Endocrine (2017) 56:379–387
DOI 10.1007/s12020-016-1044-0

ORIGINAL ARTICLE

The expression of monocarboxylate transporters in thyroid carcinoma can be associated with the morphological features of *BRAF*^{V600E} mutation

Esther Diana Rossi[1] · Tommaso Bizzarro[1] · Sara Granja[2,3] · Maurizio Martini[1] · Sara Capodimonti[1] · Emilia Luca[1] · Guido Fadda[1] · Celestino Pio Lombardi[4] · Alfredo Pontecorvi[5] · Luigi Maria Larocca[1] · Fatima Baltazar[2,3] · Fernando Schmitt[6,7,8]

Received: 22 March 2016 / Accepted: 29 June 2016 / Published online: 2 August 2016

Abstract *BRAF*^{V600E} mutation, usually performed by DNA techniques, is one of the most common diagnostic markers in papillary thyroid carcinoma. Few papers have demonstrated that plump cells (eosinophilic cytoplasms and papillary thyroid carcinoma nuclei) and peculiar sickle-shaped nuclei represent morphological features of *BRAF*^{V600E} on papillary thyroid carcinomas. These features seem to be linked to glycolytic phenotype whereby monocarboxylate transporters 1–4 are hypothesized to have a dominant role as lactate transporters. We investigated the association between these morphological features and monocarboxylate transporters 1 and 4 in 48 cyto-histological samples diagnosed as "positive for malignancy-favoring papillary thyroid carcinoma". These cases were processed with liquid-based cytology and underwent *BRAF*^{V600E} mutational analysis (pyrosequencing) on liquid-based cytology and monocarboxylate transporters immunostaining on histology. The expression of monocarboxylate transporter 1, monocarboxylate transporter 4, glucose trasporter-1 and carbonic anhidrase were scored semi-quantitatively with expression from 0 to 3+ (strong positivity). The 33 mutated and 15 wild type cases showed 100 % cyto-histological concordance. The cytological evaluation revealed plump cells and sickle nuclear shape in 100 % mutated cases. Monocarboxylate transporter 1 yielded 76 % positivity in the mutated cases especially in both the plump cells and sickle-shaped nuclei, whereas the wild types showed 13.3 % positive monocarboxylate transporter 1 ($p = 0.00013$). Monocarboxylate transporter 4 resulted in 100 % positivity in mutated and 40 % in wild types ($p < 0.005$). Furthermore, 20 % of the wild types showed weak monocarboxylate transporter 1 nuclear expression associated to a less aggressive behavior. The analysis of glucose trasporter-1 and carbonic anhidrase did not highlight any statistical significance ($p > 0.05$). This is the first report analyzing the association between monocarboxylate transporter expression and the morphological features of *BRAF*^{V600E} mutated papillary thyroid carcinomas suggesting the possible involvement of lactate in the morphological features.

Keywords Liquid-based cytology · Thyroid lesions · PTC · Plump cells · MCTs · *BRAF*^{V600E} mutation

Electronic supplementary material The online version of this article (doi:10.1007/s12020-016-1044-0) contains supplementary material, which is available to authorized users.

The preliminary data of this project were presented as a poster at the 104th USCAP meeting in Boston, 21–27 March 2015

Luigi Maria Larocca, Fatima Baltazar and Fernando Schmitt shared senior authorship.

✉ Esther Diana Rossi
esther.rossi@rm.unicatt.it

1 Division of Anatomic Pathology, Catholic University of Sacred Heart-Rome, Milano, Italy

2 Life and Health Sciences Research Institute (ICVS), School of Health Sciences, University of Minho, Braga, Portugal

3 ICVS/3B's-PT Government Associate Laboratory, Braga/Guimarães, Portugal

4 Division of Endocrine surgery, Catholic University-Rome, Milano, Italy

5 Division of Endocrinology Catholic University-Rome, Milano, Italy

6 Medical Faculty/University, Porto, Portugal

7 Institute of Pathology/Molecular Immunology of Porto, Porto, Portugal

8 Laboratorie National de Sante-Luxembourg, Luxembourg, Luxembourg

Introduction

In the last years, several papers have demonstrated that well differentiated thyroid carcinomas, mainly the classical variant of papillary thyroid carcinoma (PTC) harbors activating somatic mutations in v-raf murine sarcoma viral oncogene homolog B (*BRAF*) oncogene as demonstrated by its 45–70 % prevalence in PTCs with also prognostic implications [1–5]. Among all *BRAF* mutations, more than 95 % of them involve the exon 15 of the B isoform of *RAF kinase* gene resulting in a valine to glutamic acid substitution in the BRAF protein $BRAF^{V600E}$ [1–8]. However several entities, including the majority of follicular variants (FVPC), follicular and Hurthle cell carcinomas are devoid of this mutation [1–7]. Furthermore the diagnostic and prognostic significance of $BRAF^{V600E}$ mutation in PTCs and/or its variants is less clear and defined even if a recent multicenter retrospective review confirmed highly significant increased risk of recurrence, multifocal carcinomas, lymph-node metastases, and extrathyroidal extension in $BRAF^{V600E}$ mutated PTC on FNA [8].

Despite the invaluable advantages of DNA-based methods to assess somatic mutations, the recognition of either the novel monoclonal $BRAF^{V600E}$ antibody (clone VE1) or the new insights of the morphological features associated with $BRAF^{V600E}$ mutation are now subject to increased investigations [8–15]. Nonetheless, to date, only three papers, including one from our group, emphasized that these distinctive morphological features including some architectural (tumor-associated stromal reaction, infiltrative tumor borders) and cellular specific parameters (polygonal eosinophilic cells defined as "plump cells" and sickle-shaped nuclei) are likely to show high predictive value for $BRAF^{V600E}$ mutation in PTCs [12–15]. Nevertheless, the molecular mechanism beneath these morphological findings in thyroid carcinomas is not completely known. However, as previously demonstrated by Hall et al. in $BRAF^{V600E}$ melanoma cell lines, they pointed to the "Warburg effect" pioneering the ability of $BRAF^{V600E}$ cancer cells to uphold the activity of glycolysis providing evidence that oncogene addiction rests on a strikingly different energetic metabolism. This aerobic glycolysis implies the conversion of pyruvate to lactic acid leading to a reduction in intracellular pH [16–18].

The resulting lactate accumulation in $BRAF^{V600E}$ mutated cells may justify the morphological findings of abundant eosinophilic cytoplasm shared by these cells [19, 20]. In this perspective, monocarboxylate transporters (MCTs), especially the first 4MCTs (MCT1–4), glucose trasporter-1 (GLUT1), and pH regulator (carbonic anhidrase—CAIX), play a main role in transporting lactate and other monocarboxylates across membranes coupled with a proton as well as in contributing to the extrusion of lactate and the maintenance of the intracellular pH of tumor cells [21–27]. Despite the fact that the role of MCTs is still far from being fully defined in cancer, Pinheiro et al. provided some information in several human tumors like from brain, breast, sarcomas, uterine cervix [21–27]. Herein, we investigate the correlation between the morphological findings associated with $BRAF^{V600E}$ and MCTs in 48 thyroid cytological cases diagnosed as "positive for malignancy" and followed by surgical outcome.

Material and methods

We included all the 48 "positive for malignancy-favoring PTC (PM)" samples with surgical follow-up in the period between January 2013 and December 2013 and recorded in the Division of Pathology in Rome. All Fine needle aspiration cytology (FNAC) were carried out under-sonographic guidance (US) mostly by surgeons and endocrinologists and processed with liquid-based cytological (LBC) Thin Prep 5000™ method (Hologic Co., Marlborough, MA).

Our patients were studied with US during their thyroid check-up performed in the "Centre for Thyroid Diseases" of our hospital. The series included 12 male and 36 female patients with a median age of 27 years (range 19–73 years old). All aspirations (usually two passes for each lesion) were performed with 25–27 G needles; no rapid on-site assessment of the adequacy of the material was done. All patients had been appropriately informed regarding the use of LBC method for processing their samples and a written informed consensus was signed. Our study followed the tenants of the Declaration of Helsinki receiving the internal (Catholic University) ethical approval for the study. The resulting LBC slides were fixed in 95 % methanol and stained with Papanicolaou, while the remaining material is stored in the Preservcyt™ solution to be used for the preparation of additional slides for further investigations [including both immunocytochemistry (ICC) and molecular analysis] as described in our previous papers [11, 14, 28].

The lower limit for the adequacy for each sample was established according to the British RCPath classification, in six groups of thyroid follicular epithelial cells within the submitted LBC slides, each of them with at least 10 well-visualized epithelial cells [29].

The cytological cases were classified according to the Italian classification which shares several categories with the Bethesda System for Reporting Thyroid Cytopathology [30, 31]. All the cytological and histological diagnoses were evaluated by two expert pathologists (EDR, GF) and those cases whose interpretation was equivocal were submitted to the diagnostic judgment of the other pathologists until a final agreement was achieved. According to the definition of

plump cells, previously described in our paper and characterized by neoplastic cells displaying homogenous eosinophilic cytoplasms and with their height which was less than twice their width, we excluded both cases diagnosed as tall cell variant (TCV) and oxyphilic variant of PTC. Specifically, the former entity shows the peculiar predominance of neoplastic PTC cells whose height was at least three times their widths, while the latter entity was characterized by distinctive neoplastic atypical cells with oxyphilic basal zone, mid-placed nuclei, and slightly clearer apical region contrasting the homogeneous eosinophilic cytoplasms of plump cells.

Molecular analysis

DNA was extracted from LBC samples stored in PreserveCyt® solution (Hologic, Marlborough, MA, USA) and from paraffin embedded tissues. The specific details of our molecular method on LBC and histology have been accurately detailed in our previous papers [11, 14, 28, 32]. Sensitivity of this method states 5 % in our laboratory. The following sequence was analyzed: Exon 15: ACAGT/AGAAA. The percentage of disease specific cells for molecular analysis was at least 50 % in all LBC samples. The *BRAF* mutational analysis was also performed on DNA extracted by surgical specimens, containing at least 70 % of tumor.

Histology

All surgical specimens were fixed in 10 % buffered formaldehyde, embedded in paraffin and the 5 micron-thick microtomic sections were stained with hematoxylin and eosin. All the peri-thyroid adipose tissue was embedded and examined for the lymph-node research. The diagnosis of PTC was based on the presence of true papillary structures and the distinctive nuclear features, whereas the diagnosis FVPC relied upon the detection of the nuclear features of PTC in multiple foci within the tumor including both diffuse and encapsulated variants [33]. Encapsulated tumors with either lympho-vascular invasion (within the capsule or beyond) or capsular penetration were diagnosed as invasive FVPCs. TCV was characterized by predominance of neoplastic cells whose heights were at least three times their widths and with classical PTC nuclear features. The oxyphilic variant of PTC was defined by distinctive neoplastic cells showing marked cellular atypia with oxyphilic basal zone, mid-placed nuclei, and slightly clearer apical region. All cases were classified according to the seventh edition of the tumor-node-metastasis-based staging system recommended by the American Joint Commission on Cancer (AJCC) [33].

Immunohistochemistry

We retrospectively analyzed all the 48 histological specimens for MCT expression. Immunohistochemistry for MCT1 was performed according to the avidin-biotin-peroxidase complex method (R.T.U. VECTASTAIN Elite ABC kit (Universal), Vector Laboratories, Burlingame, CA) with primary antibodies for MCT1 (AB3538P Chemicon International), while MCT4, GLUT1, and CAIX immunostaining was done according to the streptavidin-biotin-complex principle (Ultravision Detection System Anti-polyvalent, HRP, LabVision Corporation, Fremont, CA) with primary antibodies for MCT4 (sc-50329 Santa Cruz Biotecnology), GLUT1 (ab15309-500 AbCam), and CAIX (ab15086 AbCam) diluted as previously described (Table 1, [21–26]). Negative controls were performed by the use of appropriate serum controls for the primary antibodies, whereas colon cancer and kidney were used as positive controls. Reactions were evaluated by two pathologists (EDR, FS) blinded to the *BRAF* molecular status and discordant results were discussed in a multi-head microscope.

The interpretation and validation of application on histology were supported by our previous experience [21–26]. Briefly, the cytoplasm and plasma membrane positivity of the samples was scored semi-quantitatively as follow: 0:0 % of cells; 1:<5 % positive cells; 2:5–50 % positive cells; 3:>50 % positive cells. Also intensity of staining was scored semi-qualitatively as follows: 0:negative; 1:weak; 2:intermediate; 3:strong. The final score was rendered as the sum of both parameters and grouped as negative (score 0–2) and positive (score 3–6).

Statistical analysis

Statistical analysis was performed by using a commercially available statistical software package (SPSS23, Chicago, IL, USA) for Windows (Microsoft, Redmond, Washington, USA). Comparison of categorical variables was performed by χ^2 statistic, using the Fisher's exact test when appropriate. A p value lower than 0.05 was considered significant.

Results

All the 48 cyto-histological samples diagnosed as "positive for malignancy" in the period between January and December 2013 were analyzed for the expression of the

Table 1 Description of the immunomarkers

Peptide/protein target	Antigene sequence (If known)	Name of antibody	Manufacturer	Dilution used
AB3538P chemicon international	—	Monocarboxylate 1 (MCT1)	Vector Laboratories-Burlingame-CA	1:200
sc-50329 Santa Cruz Biotecnology	—	Monocarboxylate 4 (MCT4)	LabVision Corporation-Fremont-CA	1:500
ab15309-500 AbCam	—	glucose trasporter-1 (GLUT1)	LabVision Corporation-Fremont-CA	1:100
ab15086 AbCam	—	carbonic anhidrase-CAIX	LabVision Corporation-Fremont-CA	1:100

Table 2 Clinical-pathological data of PTCs' patients

Clinical features	$BRAF^{V600E}$ *n* (%)	BRAF WT *n* (%)
Sex		
Male	7 (21.2 %)	5 (33.3 %)
Female	26 (78.8 %)	10 (66.7 %)
Age range (median)		
	24–74 (45 y.o.)	27–78 (46 y.o.)
Size		
<2 cm	30 (91 %)	12 (80 %)
>2 cm	3 (9 %)	3 (20 %)
Cytology		
TIR5	33	15
Histology		
PTC	31 (94 %)	12 (80 %)
FVPTC	2[a] (6 %)	3[a] (20 %)
T-stage		
TI–TII	23 (69.7 %)	8 (53.3 %)
TIII–TIV	10 (30.3 %)	7 (46.7 %)
N-stage		
pNO	22 (66.6 %)	9 (60 %)
pN1	11 (33.4 %)	6 (40 %)
Plump cells		
Absent	0	11
Focal	3	4
Diffuse	30	0
Sickle-shaped nuclei		
Present	33	0

All the parameters were not statistical significant ($p > 0.05$)

y.o. years old, *WT* wild type, *PTC* papillary thyroid carcinoma, *FVPC* follicular variant of PTC, *TIR5* positive for malignancy, *T-stage* tumor stage, *N-stage* lymph-node stage

[a]All the 2 $BRAF^{V600E}$ mutated FVPCs and 1 WT FVPC were invasive FVPCs

MCT isoforms 1 and 4 as well as CAIX and GLUT1. Table 2 shows the distribution of clinical-pathological features in the 33 mutated (69 %) and 15 WT cases (31 %). Regardless of $BRAF^{V600E}$ mutation, 42 out of 48 nodules resulted as equal as or smaller than 2 cm size. All the cases were histological confirmed and diagnosed as 43 classical variant of PTC and 5 FVPC of papillary thyroid cancer (including three invasive FVPCs and two encapsulated FVPCs). The distribution of these histological diagnoses between mutated and WTs is reported in Table 2. We excluded all the cases resulted as TCV and oxyphilic PTC at histology as indicated in the "Material and methods" section. Moreover, T-stage (subdivided into into TI–TII and TIII–TIV) and N-stage did not reach statistical significance in the two groups. Lymph-node metastases were found in 11 out of 33 (33.4 %) $BRAF^{V600E}$ mutated cases and in 6 out

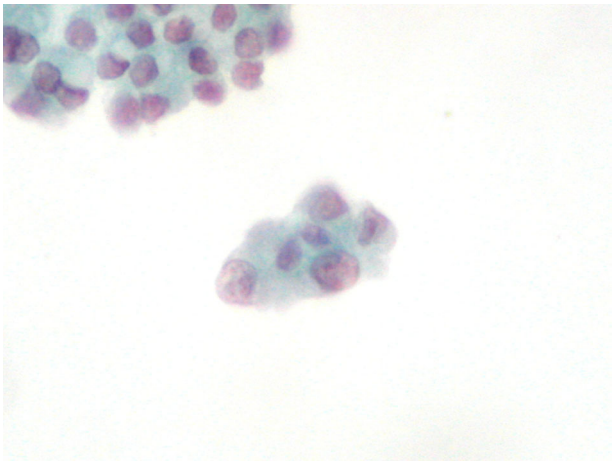

Fig. 1 Cytological sample of a $BRAF^{V600E}$ mutated cases diagnosed as "positive for malignancy-favoring PTC". Evidence of plump cells with eosinophilic cytoplasms and nuclear features of PTC and evidence of sickle-shaped nuclei on LCB (LBC, 40X)

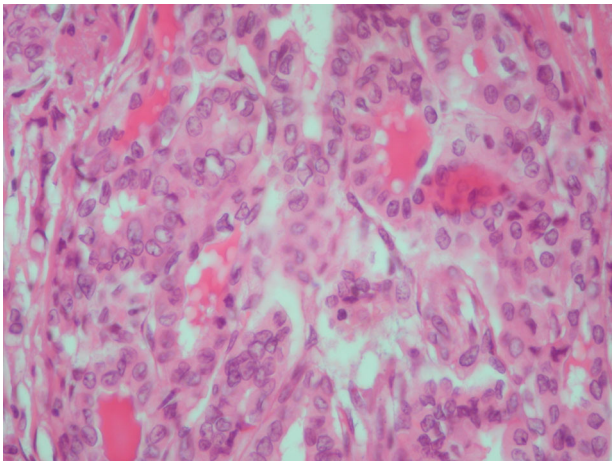

Fig. 2 Histological sample from the same cytological case with specific histological details of plump cells with details on the sickle-shaped nuclei (H&E 60X)

of 15 (40 %) WTs. As underlined in Table 2, there were no statistical significant differences in any of the analyzed parameters ($p > 0.05$). According to our purpose, we sought for both the typical nuclear features of papillary thyroid carcinoma (grooves, pleomorphic membrane, and nuclear pseudo-inclusions) and the recently described "plump cells" showing the morphological features of polygonal cells with abundant eosinophilic cytoplasm (Figs. 1 and 2, 14, 15). Furthermore, the quantification of the plump cell component proves that these cells are significantly associated with $BRAF^{V600E}$ mutation ($p = 0.0002$-OR 70.23 95 % CI 3.46–1.427) with only 3 out of 33 (9 %) mutated cases incurring focal plump cell component belonging to the PTC histotype [14]. Moreover, we reported 4 out of 15 (27 %) WT samples with focal plump cell components (Table 1) diagnosed as PTCs. Sickle-shaped nuclei were found in 100 % of our mutated $BRAF^{V600E}$ and absent in WTs (Table 2). We reported 100 % concordance for the same peculiar parameters in the corresponding histological sections (Fig. 1). In the group of FVPCs, the two mutated invasive FVPCs showed both diffuse plump cells and sickle-shaped nuclei while none of the WT FVPC (diagnosed as two encapsulated and 1 invasive FVPCs) had these morphological parameters.

Table 3a shows the results of IHC expression for the metabolism-related markers. We focused our attention on the correlation between these immunomarkers and $BRAF^{V600E}$ mutation. In keeping with our previous yields, we confirmed that the IHC expression of these proteins was found at the plasma membrane in all the cases but 3 WT cases with nuclear expression of MCT1. Specifically, MCT1 was found positive in 27 cases including 25 mutated carcinomas (detailed in the table for histotypes) and 2 WTs. Moreover, the correlation of ICC expression with the morphological findings of plump cells and sickle-shaped nuclei showed moderate to strong MCT1 expression in both plump cells and sickle-shaped nuclei of all mutated cases (Fig. 3); on the other hand, only one WT case with focal plump cells expressed MCT1. Additionally, all the normal thyroid tissue around the carcinomas showed negative IHC expression for these immunomarkers. In detail, the perineoplastic thyroid tissue presented 8 hyperplastic nodules and 2 small follicular adenomas with negative IHC expression.

The analysis of MCT4 showed 100 % positivity in mutated cases and 40 % WTs (histotype details in the Table 3a). The expression was both on the plasma membrane and cytoplasm. In the majority of mutated cases we found a strong expression (3+) in more than 50 % of the plump cells and sickle-shaped nuclei (Fig. 4). In the WT group, apart from four cases with focal plump cells showing strong expression (3+), we found two additional cases with moderate expression (2+) in less than 5 % of the cells.

The analysis of CAIX (Fig. 5) and GLUT1 (Fig. 6) (plasma membrane and cytoplasm) expression was devoid of statistical significance as demonstrated by similar positivity in 79 % of the 33 mutated, as well as in 87 % of WTs for the former while GLUT1 was positive in the majority of cases (88 % mutated and 67 % WTs). We also worked out that MCT1 demonstrated the highest specificity (86.7 %) and positive predictive value (PPV-92 %) while MCT4 showed 100 % sensitivity and 100 % negative predictive value (NPV). Lower values have been associated with CAIX and GLUT1 (specificity ranging from 13.3 to 33.3 %; NPV between 22.2 and 55.6 % and diagnostic accuracy between 58.3 and 70.8 %).

In Table 3b, we show the statistical significance of the combination of these immunomarkers. In this regard, we underscored that all our 33 mutated cases expressed

Table 3a Association of MCT1, MCT4, CAIX, and GLUT1 expression in thyroid samples

	MCT1		MCT4		CAIX		GLUT1	
	+	−	+	−	+	−	+	−
PTC								
BRAF^{V600E}	24 (77.5 %)	7 (22.5 %)	31 (100 %)	0 (0 %)	25 (80.6 %)	6 (19.4 %)	28 (90.3 %)	3 (9.7 %)
BRAF WT	1 (8.3 %)	11 (91.7 %)	6 (50 %)	6 (50 %)	11 (91.7 %)	1 (8.3 %)	8 (66.7 %)	4 (33.3 %)
FVPTC								
BRAF^{V600E}	1 (50 %)	1 (50 %)	2 (100 %)	0 (0 %)	1 (50 %)	1 (50 %)	1 (50 %)	1 (50 %)
BRAF WT	1 (33.3 %)	2 (66.7 %)	0 (0 %)	3 (100 %)	2 (66.7 %)	1 (33.3 %)	2 (66.7 %)	1 (33.3 %)

WT wild type, *PTC* papillary thyroid carcinoma, *FVPC* Follicular variant of PTC

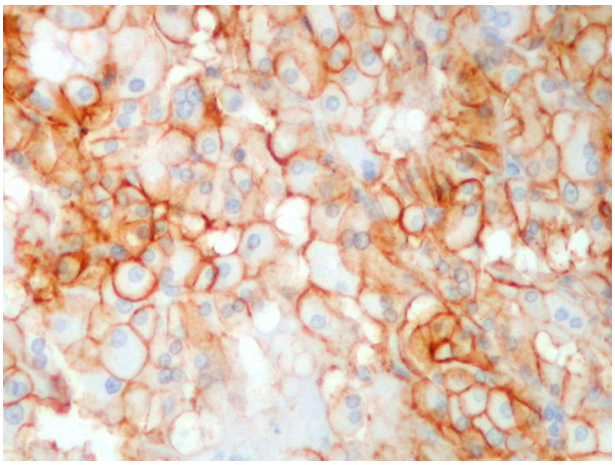

Fig. 3 Positive (plasma membrane) expression of MCT1 in the same *BRAF*^{V600E} mutated PTC (ABC 400X)

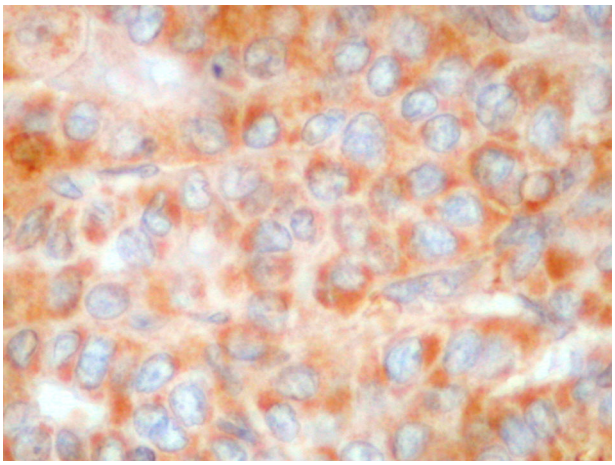

Fig. 5 Positive (plasma membrane and cytoplasm) expression of CAIX in the same *BRAF*^{V600E} mutated PTC (ABC 400X)

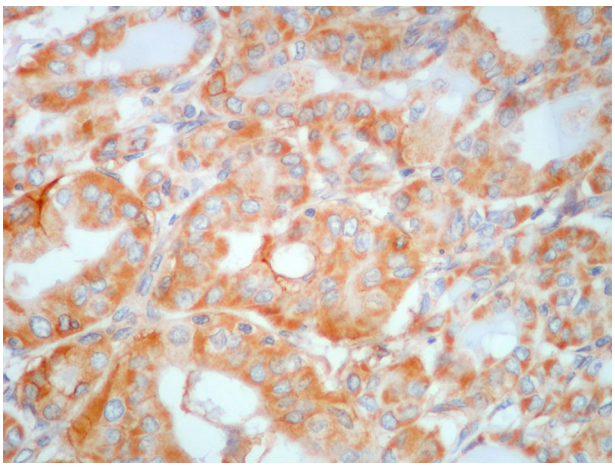

Fig. 4 Positive (plasma membrane and cytoplasm) expression of MCT4 in the same *BRAF*^{V600E} mutated PTC (ABC 400X)

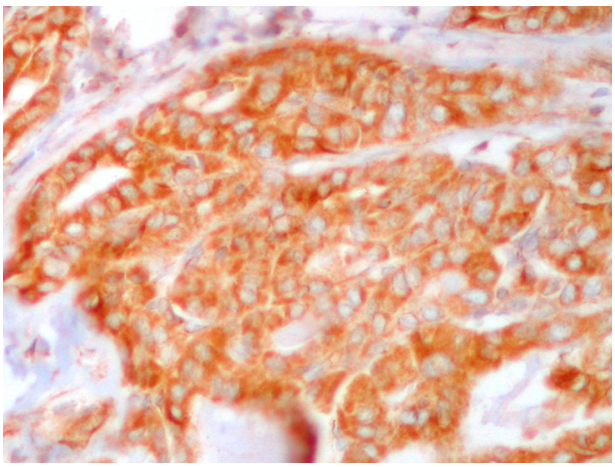

Fig. 6 Positive (plasma membrane and cytoplasm) expression of GLUT1 in the same *BRAF*^{V600E} mutated PTC (ABC 400X)

positivity in more than two immunomarkers, while among the WTs only 4 out of 15 (26 %) had a combined score equal to or greater than three markers. The specific distribution of ICC markers in both mutated and WT cases is detailed in Table 3b.

Regarding the correlation between the clinical–pathological features and the expression of the immunomarkers, we analyzed their implication with some aggressive parameters, including multifocality, extrathyroid infiltration, and lymph-node metastases; however, none of

the markers reached statistical significance as highlighted in Table 4 ($p > 0.05$). Firstly, despite the lack of statistical correlation, we saw that MCT1 and GLUT1 expression was associated with lymph-node metastases in 59 and 88.2 % of the cases, respectively. No significant associations were found for CAIX and MCT4 (Table 4). However, the data highlighted a slightly higher percentage of positive cases among the cases with higher T-stage (TIII–TIV), metastatic lymph nodes (pN1) and multifocality (Table 4).

Discussion

The aim of our paper is to evaluate the correlation between specific morphological features of $BRAF^{V600E}$ mutation previously described on PTCs and the alteration of lactate metabolism through the expression of MCTs and other metabolism-related proteins.

To date, only few papers have investigated and demonstrated that PTCs with $BRAF^{V600E}$ mutation have distinctive morphological features (specifically plump cells and sickle-shaped nuclei) which may be easily detected on cytological and histological samples of thyroid malignant lesions [12–15]. In fact, in two different papers, Virk et al. and Finkelstein et al. identified the presence of large polygonal tumor cells with homogeneous, eosinophilic, moderate to abundant cytoplasm with nuclear features of PTC in 72 and 65 % of their $BRAF^{V600E}$ mutated PTCs, respectively [12, 13].

According to the data provided by Virk et al. and Finkelstein et al., we identified the same plump cells in all the cases harboring $BRAF^{V600E}$ in both malignant cytological and histological thyroid specimens including PTCs and invasive FVPCs. Notably, in doing so, we discovered a peculiar sickle shape nuclear morphology in all the $BRAF^{V600E}$ cases that neither Virk nor Finkelstein had previously described or reported this finding in their thyroid lesions [14, 15]. It is noteworthy that our WTs cases were completely devoid of these pathognomonic shaped nuclei. To determine which mechanisms were most essential for those morphological features, the examination of a possible involvement of metabolic changes has been suspected. However, the explanation of the molecular mechanisms beneath these predictive features of mutation is unlikely to be completely understood. Since cancer cells up-regulate glucose metabolism to induce aerobic glycolysis with the so-called Warburg effect, this may be the springboard of the possible correlation with altered metabolism in these "plump" cells and $BRAF^{V600E}$ mutation [17–20].

Using $BRAF^{V600E}$ melanoma cell lines, Hall et al. demonstrated the addiction to the glycolytic metabolism promoted by mutated oncogenes through the active signaling pathway driving the up-regulation of genes involved in glycolysis [17–20]. Equally importantly, the hyperglycolytic phenotype may pave the way for the use of new tailored therapeutic strategies in clinical trials of patients with resistance to radio-iodine therapies.

Therefore we decided to shed light on the hypothesis of hyperglycolytic phenotype in mutated PTCs by the investigation of MCTs. Specifically MCT1 and MCT4, are the main proteins responsible for the extrusion of lactate, being their activity essential for the maintenance of the glycolytic phenotype. In previous reports, the functional role of MCTs have been revealed as mediating the extrusion of lactate and

Table 3b Combined positive immunomarkers in the 48 samples. Only plasma membrane expressions were considered

	$BRAF^{V600E}$	BRAF WT
4 positive IM	19	1
3 positive IM	9	3
2 positive IM	5	8
1 positive IM	0	2
0 positive IM	0	1

IM immunomarkers

Table 4 Association of MCT1, MCT4, CAIX, GLUT1 with prognostic/aggressive parameters

	MCT1		MCT4		CAIX		GLUT1	
	+	−	+	−	+	−	+	−
T-stage								
TI–TII	16 (51.6 %)	15 (48.4 %)	25 (80.6)	6 (19.4 %)	24 (77.4 %)	7 (22.6 %)	25 (80.6 %)	6 (19.4 %)
TIII–TIV	9 (53 %)	8 (47 %)	14 (82.3 %)	3 (17.7 %)	15 (88.2 %)	2 (17.8 %)	14 (82.3 %)	3 (17.7 %)
N-stage								
pN0	15 (48.4 %)	16 (51.6 %)	25 (80.6 %)	6 (19.4 %)	26 (83.8 %)	5 (16.2 %)	24 (77.4 %)	7 (22.6 %)
pN1	10 (58.8 %)	7 (41.2 %)	14 (82.3 %)	3 (17.7 %)	13 (76.5 %)	4 (23.5 %)	15 (88.2 %)	2 (11.8 %)
Multifocality								
Absent	12 (54.5 %)	10 (45.5 %)	16 (72.7 %)	6 (27.3 %)	17 (77.3 %)	5 (22.7 %)	16 (72.7 %)	6 (27.3 %)
Present	13 (50 %)	13 (50 %)	23 (88.5 %)	3 (11.5 %)	22 (84.6 %)	4 (15.4 %)	23 (88.5 %)	3 (11.5 %)

also contributing to the maintenance of the intracellular pH of tumor cells of different body sites [21–27, 34–36].

In this regard, the previously investigated analysis of MCT expression by our group led to useful information about the prognostic impact of these proteins in several solid epithelial and mesenchymal tumors including brain, colon, breast, uterine cervix, lung even though their role in thyroid carcinomas have never been investigated [21–27, 34–36]. To the best of our knowledge this is the first study in which 48 thyroid PTCs were analyzed for the comparative analysis between MCTs and the morphological findings of $BRAF^{V600E}$ mutation. In agreement with the previous studies, we described MCT expression at the plasma membrane (MCT1) and cytoplasm of mutated cells (MCT4), and found nuclear expression in WT cases. In fact, as previously described by Pinheiro et al. in sarcomas, also in this series we recognized the nuclear expression of MCT1, suggesting the existence of an additional role of MCT1 which may induce a less aggressive behavior in the thyroid carcinomas [21].

In the present study, both MCT1 and MCT4 highlighted a correlation with plump cells and sickle-shaped nuclei defined by 76 and 97.1 % positive expression in the mutated cases, respectively. Additionally, we documented MCT expression in cases with focal plump cells, underlying that these markers recognized specifically these morphological features and they may represent a valid aid especially on cytological samples.

Considering that the high glycolytic rates in cancer cells lead to accumulation of lactate, the increase of MCT1 and MCT4 expression in the plasma membrane of plump cells would support the glycolytic phenotype ending with the reduction of intracellular acidosis and apoptosis. Hence, the larger number of mutated plump cells with MCT4 compared to those with MCT1 may justify the different role of these proteins, as previously clarified [21].

In fact, MCT1 is considered an intermediate affinity isoform while MCT4 is a low affinity transporter, which expression has been observed in highly glycolytic tissues where it is responsible for lactate efflux [36]. The detection of strong and diffuse MCT4 expression in mutated thyroid PTCs could avoid cellular acidification and, as a consequence, promote cell survival and prevention of apoptosis. In this regard, we also combined these markers with the clinic-pathological diagnoses in order to investigate a possible prediction of their prognostic value. In this perspective, and as previously done in other papers, we compared the expression of these markers with T-stage, N-stage, and multifocality. Nonetheless, the evidence that both MCT1 and MCT4 were able to distinguish between groups with worse and better prognosis was not appreciated in the present work. In fact, we only found a slightly larger number of MCT1 positive cases with extrathyroid extension (TIII–TIV) while all the analysis of the remaining 3 markers did not show any statistical significance. Despite the limited number of cases in our series, this lack of prognostic correlation may imply that, in PTCs, the role of these transporters is linked to *BRAF* mutation, constituting attractive targets for cancer tailored therapies.

Concerning CAIX and GLUT1, we did not find any significant results allowing the discrimination between mutated vs. wild type cases. Specifically CAIX, which is a HIF-1α(hypoxia-inducible factor 1) target protein as well as MCT4, overlapped the result of MCT4 expression, highlighting the same semi-quantitative results in plump cells and sickle-shaped nuclei. Actually, the high number of WT cases with CAIX expression is likely to demonstrate that this protein is not regulated by the same mechanisms as MCTs. Moreover, despite the statistical significance of GLUT1 reported in mesotheliomas vs. reactive mesothelial cells [25], we did not parallel the same significant result in our mutated plump cells vs. WTs. Despite the fact that these molecular mechanisms are not object of our current paper, these results clearly support the fact that molecular mechanisms underlying MCTs need additional studies as long as MCTs seem to be induced by protein kinase C (PKC) signaling pathway while MCT1 inhibited by PKA signaling pathway [27].

In order to overcome the issues of the results obtained with single immunomarkers, we assessed the correlation between the morphological features and the entire panel of immunomarkers. Our data led to the conclusion that the majority of mutated cases had at least two positive immunomarkers, while there were not a significant number of WTs with more than two positive markers. Together, the best choice to support the morphology of plump cells seems to be ascribed to the combined use of MCT1 and MCT4 expression. In fact, these two immunomarkers provided the highest sensitivity and specificity, pointing to the preferential use of concordant positive panel rather than single markers.

This paper contributes to the suggestion that metabolic alterations also occur in $BRAF^{V600E}$ thyroid carcinomas and that the morphological features of mutation are likely to support the lactate accumulation and the potential involvement of metabolic changes through the glycolytic pathway. This first correlation between MCT expression and morphological features predictive of $BRAF^{V600E}$ mutation in PTCs may offer the possibility to study the role of specific target therapies as an additional aid. However, we are conscious that larger studies are warranted to confirm our data.

Funding This research did not receive any specific grant from any funding agency in the public, commercial or not-profit sectors.

Compliance with ethical standards

Conflict of interest The authors declare that they have no conflict of interest.

References

1. M. Xing, BRAF mutation in papillary thyroid cancer: pathogenic role, molecular bases and clinical implications. Endocr. Rev. **28**, 742–762 (2007)
2. T.H. Kim, Y.J. Park, J.A. Lim, H.Y. Ahn et al., The association of the $BRAF^{V600E}$ mutation with prognostic factors and poor clinical outcome in papillary thyroid cancer. Cancer **118**, 1764–1773 (2012)
3. M.N. Nikiforova, Y. Nikiforov, Molecular diagnostics and predictors in thyroid cancer. Thyroid **19**, 1351–1361 (2009)
4. Y.E. Nikiforov, Molecular diagnostics of thyroid tumors. Arch. Pathol. Lab. Med. **135**, 569–577 (2011)
5. V. Trovisco, I. Vieira de Castro, P. Soares et al., *BRAF* mutations are associated with some histological types of papillary thyroid carcinoma. J. Pathol. **202**, 247–251 (2004)
6. E.D. Rossi, G. Fadda, F. Schmitt, The night mare of indeterminate follicular proliferations: When liquid based cytology and ancillary techniques area not a moon landing but a concrete plan. Acta Cytol. **58**, 543–551 (2014)
7. H. Chen, I. Izevbaye, F. Chen, B. Weinstein, Recent advances in follicular variant of papillary thyroid carcinoma. N. A. J. Med. Sci. **5**, 212–219 (2012)
8. Z. Wang, J.Q. Chen, J.L. Liu, X.G. Qin, Clinical impact of BRAF mutation in the diagnosis and prognosis of papillary thyroid carcinoma: a systematic review and meta-analysis. Eur. J. Clin. Invest. **46**, 146–157 (2016)
9. C.A. Routhier, M.C. Mochel, K. Lynch, D. Dias-Santagata, D.N. Louis, M.P. Hoang, Comparison of 2monoclonal antibodies for immunohistochemical detection of $BRAF^{V600E}$ mutation in malignant melanoma, pulmonary carcinoma, gastrointestinal carcinoma, thyroid carcinoma and gliomas. Human Pathol. **44**, 2563–2570 (2013)
10. A.K. Zimmermann, U. Camerisch, M.P. Rechsteiner, B. Bode-Lesniewska, M. Rossle, Value of immunohistochemistry in detection of $BRAF^{V600E}$ mutations in fine needle aspiration biopsies of papillary thyroid carcinoma. Cancer Cytopathol **122**, 48–58 (2014)
11. E.D. Rossi, M. Martini, S. Capodimonti, B. Angrisani et al., Analysis of immunocytochemistry and molecular *BRAF* expression in thyroid carcinoma: Cyto-histological institutional experience. Cancer Cytopathol. **122**, 527–535 (2014)
12. R.K. Virk, C.G.A. Theoharis, A. Prasad, D. Chhieng, M.L. Prasad, Morphology predicts $BRAFR^{V600E}$ mutation in papillary thyroid carcinoma: an interobserver reproducibility study. Virchow Arch **464**, 435–442 (2014)
13. A. Finkelstein, G.H. Levy, P. Hui et al., Papillary thyroid carcinomas with and without $BRAF^{V600E}$ mutations are morphological distinct. Histopathology **60**, 1052–1059 (2012)
14. E.D. Rossi, T. Bizzarro, M. Martini et al., Morphologic parameters able to predict $BRAF^{V600E}$ mutated malignancies on thyroid FNAC. Our institutional experience. Cancer Cytopathol. **122**, 883–891 (2014)
15. E.D. Rossi, T. Bizzarro, G. Fadda, L.M. Larocca, F.S. Schmitt, Is morphology alone able to predict *BRAF* mutated malignancies on thyroid FNAC? Virchows Arch **465**, 247–248 (2014)
16. I. Arozarena, B. Sanchez-Laorden, L. Packer, C. Hidalgo-Carcedo et al., Oncogenic *BRAF* induces melanoma cell invasion by downregulating the cGMP-specific phosphodiesterase PDE5A. Cancer Cell **19**, 45–57 (2011)
17. A. Hall, K.D. Meyle, M.K. Lange et al., Dysfunctional oxidative phosphorylation makes malignant melanoma cells addicted to glycolysis driven by the $^{V600E}BRAF$ oncogene. Oncotarget **4**, 584–599 (2013)
18. M.H. Lee, S.E. Lee, D.W. Kim et al., Mitochondrial localization and regulation of $BRAF^{V600E}$ in thyroid cancer: a clinically used RAF inhibitor is unable to block the mitochondrial activities of $BRAF^{V600E}$. J. Clin. Endocrinol. Metab. **96**, E19–E30 (2011)
19. E. White, Exploiting the bad eating habits of RAS-driven cancers. Genes and Develop. **27**, 2065–2071 (2015)
20. A.M. Strohecker, E. White, Targeting mitochondrial metabolism by inhibiting autophagy in BRAF-driven cancers. Cancer Discov. **4**, 766–772 (2014)
21. C. Pinheiro, V. Penna, F. Morais-Santos et al., Characterization of monocarboxylate transporters (MCTs) expression in soft tissue sarcomas:distinct prognostic impact of MCT1 subcellular localization. J. Transl. Med. **12**, 118–128 (2014)
22. C. Pinheiro, A. Longatto-Filho, C. Scapulatempo et al., Increased expression of monocarboxylate transporters 1,2 and 4 in colorectal carcinomas. Virchows Arch **452**, 139–146 (2008)
23. C. Pinheiro, A. Longatto-Filho, K. Simoes et al., The prognostic value of CD147/EMMPRIN is associated with monocarboxylate transporter 1 co-expression in gastric cancer. Eur. J. Cancer **45**, 2418–2424 (2009)
24. C. Pinheiro, A. Albergaria, J. Paredes et al., Monocarboxylate transporter 1 is up-regulated in basal-like breast carcinoma. Histopathology **56**, 860–867 (2010)
25. C. Pinheiro, A. Longatto-Filho, T. Soares et al., CD147 immunohistochemistry discriminates between reactive mesothelial cells and malignant mesothelioma. Diagn. Cytopathol. **40**, 478–483 (2012)
26. C. Pinheiro, A. Longatto-Filho, S.M.M. Pereira et al., Monocarboxylate transporters 1 and 4 are associated with CD147 in cervical carcinoma. Dis. Markers **26**, 97–103 (2009)
27. K. Narumi, A. Furugen, M. Kobayashi, S. Otake, S. Itagaki, K. Iseki, Regulation of monocarboxylate transporter 1 in skeletal muscle cells by intracellular signaling pathways. Biol. Pharm. Bull. **33**, 1568–1573 (2010)
28. E.D. Rossi, M. Martini, S. Capodimonti et al., Diagnostic and prognostic value of immunocytochemistry and *BRAF* mutation analysis on liquid based biopsies of thyroid neoplasms suspicious for carcinoma. Eur. J. Endocrinol. **168**, 853–859 (2013)
29. British Thyroid Association, Guidelines for the Management of Thyroid Cancer, 2nd edn. London (2007)
30. G. Fadda, F. Basolo, A. Bondi et al.; SIAPEC-IAP Italian Consensus Working Group, Cytological classification of thyroid nodules. Pathologica **102**, 405–408 (2010)
31. E.S. Cibas, S.Z. Ali, The Bethesda system for reporting thyroid cytopathology. Thyroid **19**, 1159–1165 (2009)
32. E.D. Rossi, M. Martini, S. Capodimonti, C.P. Lombardi et al., *BRAF*(V600E) mutation analysis on LBC-processed aspiration biopsies predicts bilaterality and nodal involvement in papillary thyroid microcarcinoma. Cancer Cytopathol. **121**, 291–297 (2013)
33 American Joint Commission on Cancer (AJCC), Cancer Staging Atlas 2nd edn. Chicago (2013)
34. F. Morais-Santos, S. Granja, Miranda-Gonçalves V et al., Targeting lactate transport suppresses in vivo breast tumour growth. Oncotarget **6191**, 77–89 (2015)
35. S. Granja, I. Marchiq, R. Le Floch, C.S. Moura, F. Baltazar, J. Pouysségur, Disruption of BASIGIN decreases lactic acid export and sensitizes non-small cell lung cancer to biguanides independently of the LKB1. Oncotarget **6**, 6708–6721 (2015)
36. C. Pinheiro, A. Longatto-Filho, J. Azevedo-Silva, M. Casal, F.C. Schmitt, F. Baltazar, Role of monocarboxylate transporters in human cancers:state of the art. J. Bioenerg. Biomembr. **44**, 127–139 (2012)